



**Fermi National Accelerator Laboratory**

**FERMILAB-Conf-95/352-E**

**D0**

## **Observation of the Top Quark with the D0 Detector**

N.J. Hadley

For the D0 Collaboration

*Fermi National Accelerator Laboratory  
P.O. Box 500, Batavia, Illinois 60510*

November 1995

Submitted to the *XXIII SLAC Summer Institute on Particle Physics*,  
July 10-21, 1995

## Disclaimer

*This report was prepared as an account of work sponsored by an agency of the United States Government. Neither the United States Government nor any agency thereof, nor any of their employees, makes any warranty, expressed or implied, or assumes any legal liability or responsibility for the accuracy, completeness, or usefulness of any information, apparatus, product, or process disclosed, or represents that its use would not infringe privately owned rights. Reference herein to any specific commercial product, process, or service by trade name, trademark, manufacturer, or otherwise, does not necessarily constitute or imply its endorsement, recommendation, or favoring by the United States Government or any agency thereof. The views and opinions of authors expressed herein do not necessarily state or reflect those of the United States Government or any agency thereof.*

# **OBSERVATION OF THE TOP QUARK WITH THE DØ DETECTOR**

Nicholas J. Hadley

Physics Department

The University of Maryland, College Park, MD 20742

Representing the DØ Collaboration

at the XXIII SLAC Summer Institute on Particle Physics

July 10–21, 1995

## **ABSTRACT**

The DØ collaboration reports on the observation of top quark in  $p\bar{p}$  collisions at  $\sqrt{s} = 1.8$  TeV at the Fermilab Tevatron. We measure the top quark mass to be  $199^{+19}_{-21}(\text{stat.})^{+14}_{-21}(\text{syst.})$  GeV/c<sup>2</sup> and its production cross section to be  $6.4 \pm 2.2$  pb. Our result is based on approximately 50 pb<sup>-1</sup> of data. We observe 17 events with an expected background of  $3.8 \pm 0.6$  events. The probability of an upward fluctuation of the background to produce the observed signal is  $2 \times 10^{-6}$  (equivalent to 4.6 standard deviations). The kinematic properties of the events are consistent with top quark decay, and the distribution of events across the seven decay channels is consistent with the Standard Model top quark branching fractions. We describe the analysis that led to the observation of the top quark as well as the properties of the top quark events.

On Thursday, March 2, 1995, in two seminars given at Fermilab, the DØ and CDF collaborations announced the discovery of the top quark<sup>1,2</sup>. This discovery was the culmination of nearly two decades of intense search by a large number of different experiments located at accelerators throughout the world.

The DØ experiment measures a mass of  $199_{-21}^{+19}(\text{stat.})_{-21}^{+14}(\text{syst.})$  GeV/ $c^2$  for the top quark with a production cross section of  $6.4 \pm 2.2$  pb for that mass. (The CDF experiment measures a mass of  $176 \pm 13$  GeV/ $c^2$  and a cross section of  $6.8_{-2.4}^{+3.6}$  pb.) The DØ result is based on approximately  $50 \text{ pb}^{-1}$  of data, about four times the previous sample<sup>3,4</sup>. We observe 17 events with an expected background of  $3.8 \pm 0.6$  events. The probability of an upward fluctuation of the background to produce the observed signal is  $2 \times 10^{-6}$  (equivalent to 4.6 standard deviations). The kinematic properties of the events are consistent with top quark decay. The distribution of events across the seven decay channels we study is consistent with the Standard Model top quark branching fractions. We will describe the analysis that led to the observation of the top quark in detail, starting with a brief summary of past searches for the top quark with DØ. We will also show that our top data contains  $W$ 's that decay hadronically.

## 1 Introduction

At Tevatron energies, top quarks are primarily produced in pairs. In what follows, we assume that top quarks decay into a  $W$  boson and a  $b$  quark with 100% branching fraction. The decay modes of the top are then characterized by the decays of the two  $W$ 's in each event. Events where both  $W$ 's decay to leptons ( $e$  or  $\mu$ ) are called dilepton events, denoted  $ee$ ,  $e\mu$ , and  $\mu\mu$  events. Events where one  $W$  decays to an  $e$  or a  $\mu$  and the other decays to jets are called lepton + jets events. Decays to tau leptons are considered only as sources of jets, electrons or muons. Events where both  $W$ 's decay to jets have large backgrounds due to QCD multijet events and were not used in the discovery analysis.

In January 1994, the DØ collaboration published<sup>3</sup> an upper limit on the top quark pair production cross section which can be translated into a 95% confidence level (CL) lower limit on the top quark mass of 131 GeV/ $c^2$ . This paper used  $13.5 \text{ pb}^{-1}$  of data from the 1992–1993 run and was based on the analysis of the number of events seen in the  $ee$ ,  $e\mu$ ,  $e + \text{jets}$ , and  $\mu + \text{jets}$  decay channels.

In April 1994, the CDF collaboration submitted papers claiming evidence for

the top quark with a mass of  $174 \pm 16 \text{ GeV}/c^2$  and a cross section of  $13.9_{-4.8}^{+6.1} \text{ pb}$ . The statistical significance of the signal was about 2.8 standard deviations.<sup>5</sup>

In a paper<sup>4</sup> submitted to Physical Review Letters in November 1994, we re-optimized our analysis for higher masses, based on our previous result (top quark mass  $> 131 \text{ GeV}/c^2$ ), added more decay channels, and improved our understanding of the backgrounds in the various channels. This analysis provided a background subtracted estimate of the top quark production cross section, based on the same data set as the January 1994 paper, but using the information from all decay channels involving at least one electron or muon ( $ee$ ,  $e\mu$ ,  $\mu\mu$ ,  $e + \text{jets}$ , and  $\mu + \text{jets}$  with both event shape selection and  $b$  quark tagging). For all seven channels together, we found nine events with an expected background of  $3.8 \pm 0.9$  events. Assuming the excess to be due to  $t\bar{t}$  production, we obtained a cross section of  $8.2 \pm 5.1 \text{ pb}$  for a  $180 \text{ GeV}/c^2$  top quark mass. This cross section was consistent with both the Standard Model expectations for the top quark at this mass and with the CDF result. We concluded that this measurement did not demonstrate the existence of the top quark.

## 2 Optimization

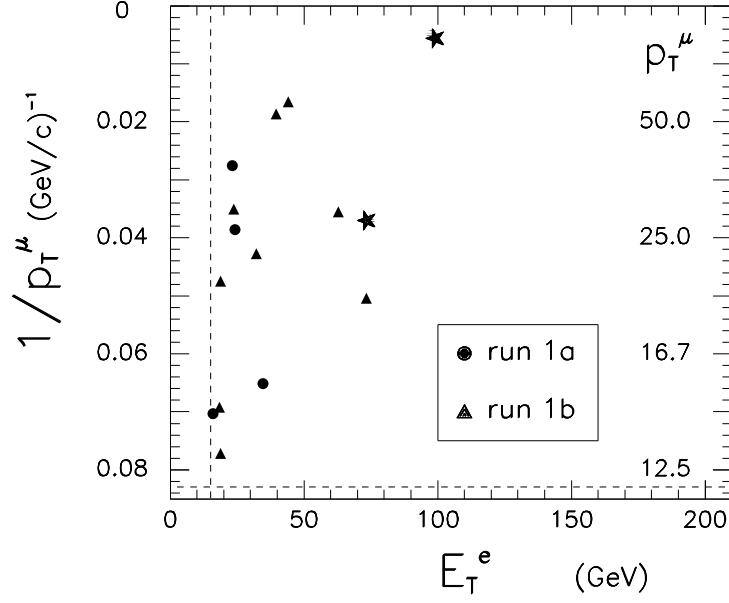
DØ began its second data run (run 1b) in December 1993, and by early 1995, we had more than tripled our data sample compared with the 1992–1993 run (run 1a). To exploit the extended mass reach of this larger data sample, about  $50 \text{ pb}^{-1}$ , we optimized our cuts for the top quark search for top masses above  $140 \text{ GeV}/c^2$ . We optimized signal to background using Monte Carlo simulations to model the signal along with our standard background calculation methods. We achieved an improvement of a factor of 4 in signal to background while retaining 70% of our previous acceptance for  $180 \text{ GeV}/c^2$  top. The improved background rejection arises primarily from requiring events to have large total transverse energy,  $H_T$ .  $H_T$  is defined as the scalar sum of the transverse energies,  $E_T$ , of the jets for the single lepton + jets and  $\mu\mu$  channels and the scalar sum of the transverse energies of the leading electron and the jets for the  $e\mu$  and  $ee$  channels. To be included in the calculation of  $H_T$ , jets were required to have  $E_T > 15 \text{ GeV}$ . Electrons are identified by their longitudinal and transverse shower shapes in the calorimeter. They are required to be isolated, to have a matching track, and to have  $dE/dx$  as measured in the tracking chambers consistent with a single electron. Electrons

are required to have  $|\eta| < 2.5$  for the dilepton channels and  $|\eta| < 2.0$  for the  $e + \text{jets}$  channels. Muons are defined by a good quality track in the muon chambers, which points to the event vertex. Muons are also required to leave a minimum amount of energy in the calorimeter. Muons are restricted to  $|\eta| < 1.7$  for data taken in the 1992–1993 run and  $|\eta| < 1.0$  for data taken in the 1993–1995 run. Due to wire aging, the muon chamber efficiency at large values of  $\eta$  decreased with time. Isolated muons were required to be more than 0.5 in  $\eta$ - $\phi$  space from the center of the nearest jet. Jets are defined using a fixed cone algorithm of radius 0.5 in  $\eta$ - $\phi$  space.

### 3 Dilepton Decay Channels

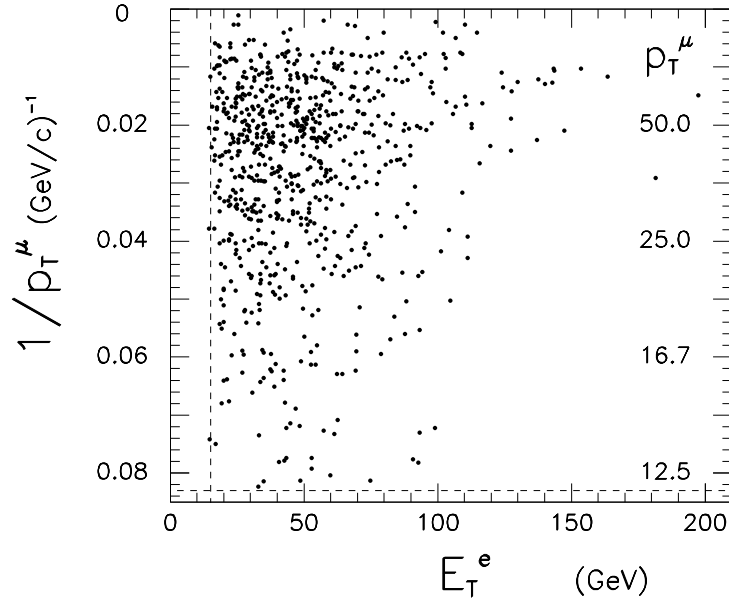
We will now describe the analysis of the seven different decay modes, starting with the dilepton channels. The branching ratios for  $t\bar{t}$  events to decay to dileptons are small, but the backgrounds are small as well. In each of the dilepton channels ( $ee$ ,  $e\mu$ , and  $\mu\mu$ ), we required two leptons, two jets, and a minimum value of  $H_T$ . In the  $ee$  and  $e\mu$  channels, we required a large missing  $E_T$ ,  $\cancel{E}_T$ , while in the  $\mu\mu$  channel, the two muons were required to be inconsistent with a  $Z$  decay based on a global kinematic fit. The kinematic requirements for the three dilepton channels are given in Table 1. After all cuts, two events remain in the  $e\mu$  channel. A plot of  $E_T^e$  vs  $1/p_T^\mu$  is given in Fig. 1. The stars in the plot show the two top candidates in this channel. Figure 2 shows a plot of  $\cancel{E}_T$  vs the invariant mass of the two electrons,  $M_{ee}$  for the  $ee$  events after the electron  $E_T$  and jet cuts. The data show a cluster of events consistent with  $Z + \text{jets}$  production. The one remaining event is removed by the  $H_T$  requirement, leaving no events in this channel. Figure 3 shows a plot of the probability that the pair of muons comes from the decay of a  $Z$  boson for  $Z \rightarrow \mu\mu$  events and for  $\mu\mu$  top events from the Monte Carlo. The location of the cut is shown by the arrow. After all cuts, one event remains in the  $\mu\mu$  channel. This event has a probability of 0.008 of coming from the decay of a  $Z$  boson. The  $H_T$  distribution of the dilepton events, along with distributions for signal and background Monte Carlo events is shown in Fig. 4. The one event with  $H_T$  below 100 GeV is the  $ee$  event that fails the  $H_T$  cut.

The backgrounds for the dilepton channels come from two sources: physics backgrounds and fake backgrounds. Physics backgrounds come from physics processes which have the same signature as top, for example  $WW \rightarrow e\mu + \text{jets}$ . These



$E_T^e$  vs  $1/p_T^\mu$

Collider Data  
 $\int \mathcal{L} dt = 47.9 \text{ pb}^{-1}$



$E_T^e$  vs  $1/p_T^\mu$

$t\bar{t} \rightarrow e\mu$  ( $m_t=170$ )  
 monte carlo  
 $\int \mathcal{L} dt = 21 \text{ fb}^{-1}$

Figure 1: Scatter plots of  $1/p_T^\mu$  versus  $E_T^e$  prior to  $H_T$ , jet, and  $\cancel{E}_T$  cuts for  $e\mu$  events from data and  $t\bar{t}$  Monte Carlo, top quark mass of  $170 \text{ GeV}/c^2$  and luminosity of  $21 \text{ fb}^{-1}$ . The dashed lines correspond to our cuts.

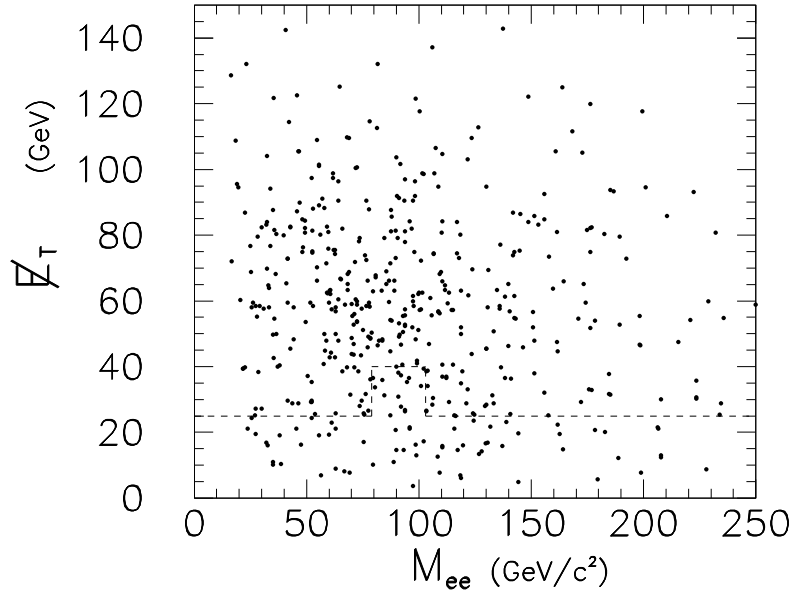
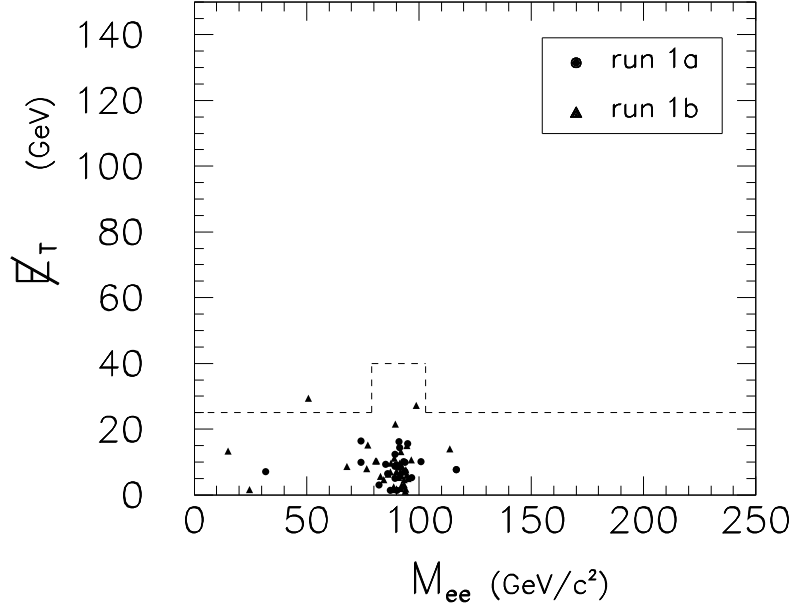


Figure 2: Scatter plots of  $E_T$  versus  $M_{ee}$  after  $E_T$  and jet cuts, but before the  $H_T$  cut for  $ee$  events from data and  $t\bar{t}$  Monte Carlo, top quark mass of 160  $\text{GeV}/c^2$  and luminosity of  $19 \text{ fb}^{-1}$ . The dashed lines correspond to our cuts.



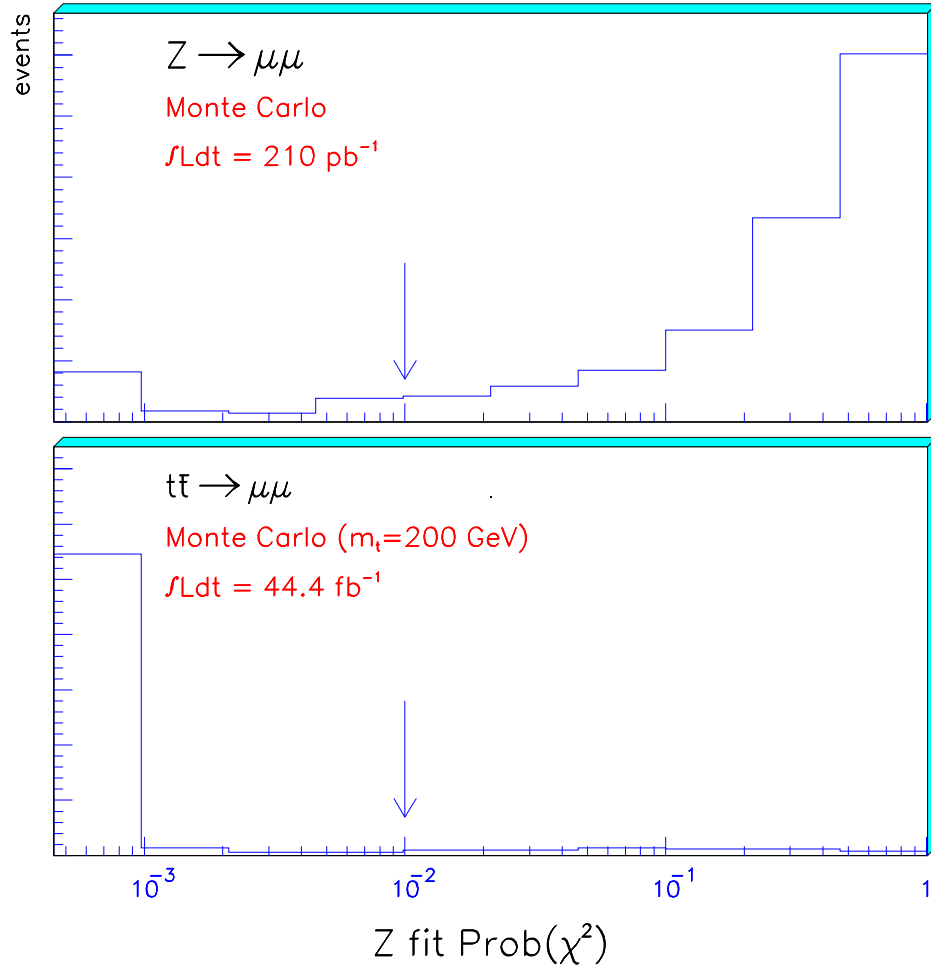


Figure 3: Plots of probability of the dimuon pair coming from the decay of a  $Z$  boson for  $Z \rightarrow \mu\mu$  and top Monte Carlo events. The location of the cut is given by the arrow.

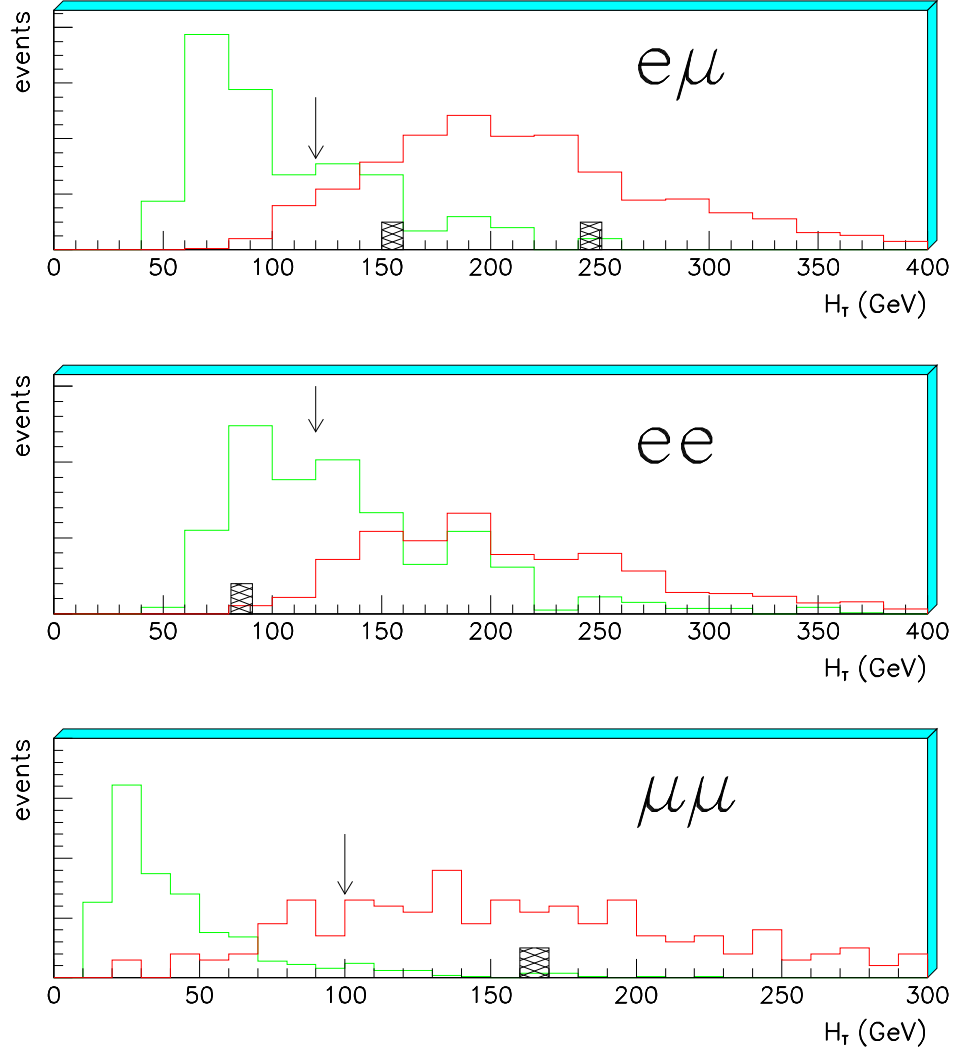


Figure 4:  $H_T$  Distribution for data events (boxes) and top (dashed lines) and background Monte Carlo events (dotted lines). The  $H_T$  distribution of the background events peaks at lower values of  $H_T$  than the top events. The arrow shows the location of the cut.

Table 1: Minimum kinematic requirements for the standard event selection (energies in GeV).

Channel	Leptons		Jets		$\cancel{E}_T$	$H_T$	$\mathcal{A}$
	$E_T(e)$	$p_T(\mu)$	$N_{\text{jet}}$	$E_T$			
$e\mu + \text{jets}$	15	12	2	15	20	120	-
$ee + \text{jets}$	20		2	15	25	120	-
$\mu\mu + \text{jets}$		15	2	15	-	100	-
$e + \text{jets}$	20		4	15	25	200	0.05
$\mu + \text{jets}$		15	4	15	20	200	0.05
$e + \text{jets}/\mu$	20		3	20	20	140	-
$\mu + \text{jets}/\mu$		15	3	20	20	140	-

backgrounds are estimated using Monte Carlo. Fake backgrounds come from processes where one object is misidentified in the detector as another object. Jets, for example, are sometimes misidentified as electrons. These backgrounds are estimated directly from data, as are the probabilities for resolution fluctuations to give large  $\cancel{E}_T$ . The main backgrounds are from  $Z$  and continuum Drell-Yan production, vector boson pairs ( $WW$ ,  $WZ$ ), heavy flavor ( $b\bar{b}$ ,  $c\bar{c}$ ) production, and backgrounds from jets misidentified as electrons. The total estimated background in all three dilepton channels is  $0.65 \pm 0.15$  events. The expected top yields are calculated using the ISAJET event generator<sup>6</sup> coupled to a GEANT<sup>7</sup> simulation of the DØ detector. With the standard cuts, we observe a total of three events. The probability of the calculated background fluctuating upward to the observed signal is 0.03. From the dilepton events alone, we calculate a top cross section of  $7.5 \pm 5.7$  pb. If we remove the  $H_T$  requirement and the cut on the probability that a pair of muons come from a  $Z$ , we have four observed events, with a calculated background of  $2.66 \pm 0.40$  events. This set of cuts without the  $H_T$  requirement is called the loose cuts. For the loose cuts, the observed cross section is  $4.4 \pm 6.8$  pb. We note that, although the statistical uncertainty is large, the cross sections obtained using the standard and loose cuts are consistent.

## 4 Lepton + Jets + Event Shape

Compared to the dilepton channels, the branching ratios are large for the lepton + jets channels, where one  $W$  decays leptonically and the other hadronically. However, the backgrounds are also large. There is a large background from  $W$  + multijet events. There is also a background from QCD multijet events where one jet fakes an electron or muon, and the missing  $E_T$  fluctuates high. We use two different methods to distinguish  $t\bar{t}$  events from background. In the first method, we exploit the different kinematics of the  $t\bar{t}$  events to separate them from the background. In the second method, we use muons near jets to tag the presence of  $b$  quark jets. A  $t\bar{t}$  event has two  $b$  jets, while background events have far fewer. We will discuss the kinematic, or event shape, method of separating top events from background first.

To separate top events in the lepton + jets channel from backgrounds without relying on the presence of a muon near a jet to tag the  $b$  jets, we note the following characteristics of the top events. Top events should have an isolated lepton, large missing  $E_T$ , and four jets. Since top is heavy, its decay products should tend to be central, and not at large rapidities. Top events should have a large value of the total transverse energy  $H_T$ , and the events should be non-planar. Here we define aplanarity,  $\mathcal{A}$ , where  $\mathcal{A} = 3/2 \times$  the smallest eigenvalue of the normalized momentum tensor constructed from the jets in the events.  $\mathcal{A} = 0.5$  for spherical events and is near 0 for planar and linear events. The kinematic requirements on the lepton + jets events are given in Table 1. The principal difference between this analysis and previous analyses<sup>4</sup> is the tighter cut on  $H_T$ . The background events from  $W$  + four jet production should have lower values of  $H_T$ . Backgrounds from multijet events where one jet fakes an electron or muon are suppressed by the missing  $E_T$  requirement and the  $\mathcal{A}$  requirement. In Fig. 5, we show the  $H_T$  distribution for Monte Carlo  $W$  + jets events and for  $t\bar{t}$  events where we assume a top mass of 200 GeV/c<sup>2</sup>. In Fig. 6 we show plots of  $H_T$  for two and three jet events where the contamination from top events is small. The agreement between our calculated background and the observed  $H_T$  distribution is good, demonstrating that we are able to calculate our backgrounds reliably. To check for possible systematic biases, we define a loose set of cuts in the lepton + jets channels as well. The loose cuts require make no requirement on  $H_T$  and require  $\mathcal{A} > 0.03$ . The standard cuts require  $\mathcal{A} > 0.05$ .

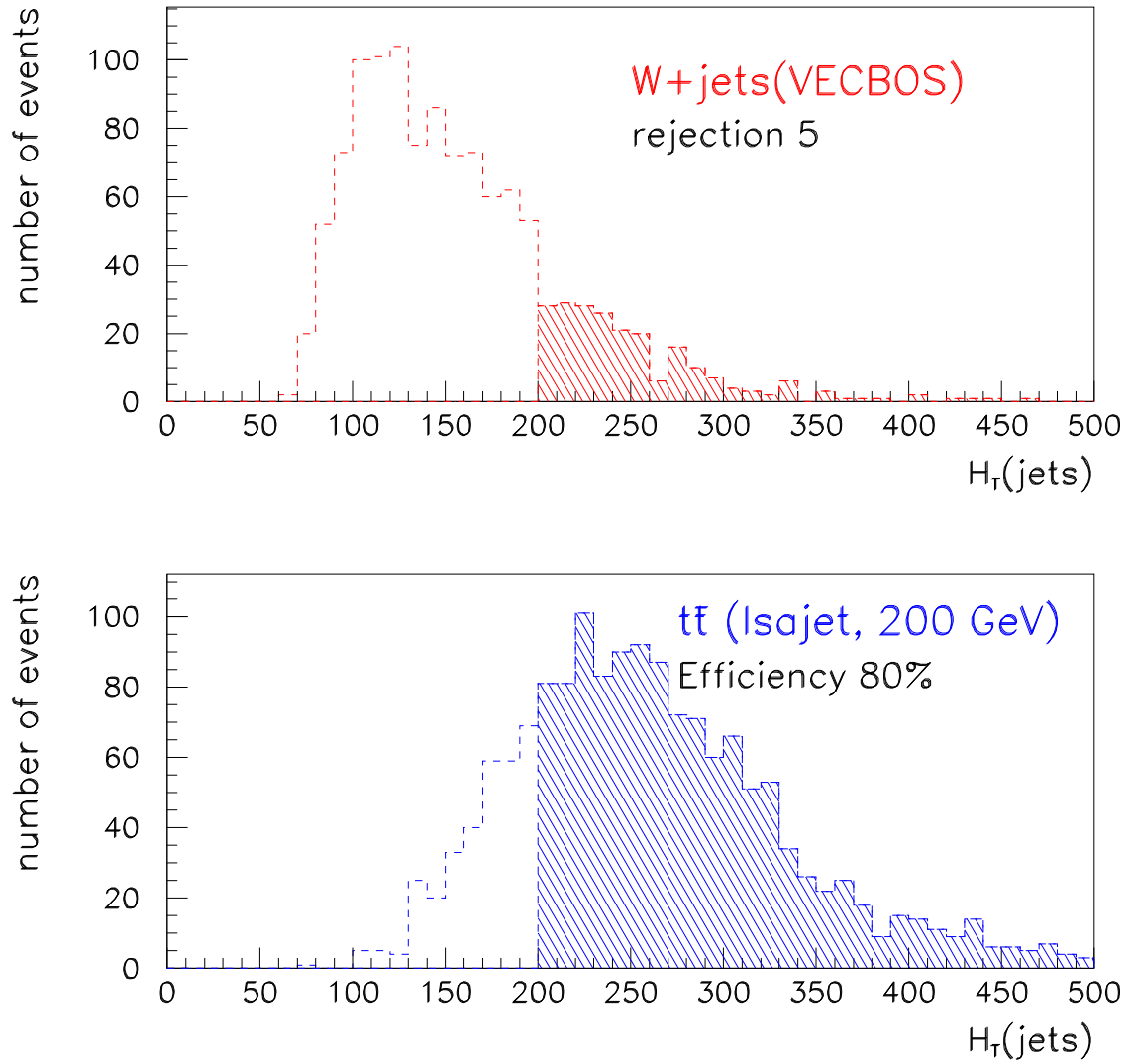


Figure 5: Plot of  $H_T$  for  $e + \text{four jet}$  events for  $W + \text{jets}$  Monte Carlo events and  $t\bar{t}$  Monte Carlo, top quark mass = 200 GeV/ $c^2$ . The shaded region is above our cut.

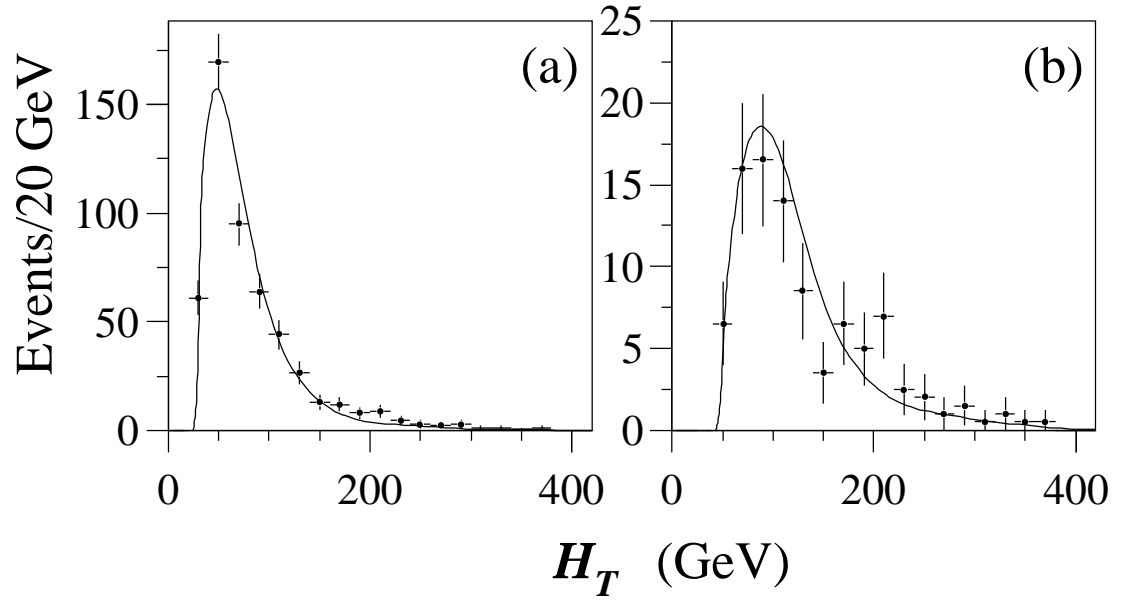


Figure 6: Plots of  $H_T$  for  $e + \text{jets}$  events with  $\cancel{E}_T > 25$  GeV. (a)  $e + \text{two jet}$  events, (b)  $e + \text{three jet}$  events. The points are data. The curves are background calculated using VECBOS and multijet data.

The backgrounds due to multijet production where a jet fakes an electron are determined from the  $\cancel{E}_T$  distribution of events containing a fake electron. Fake electrons are defined as electromagnetic clusters in the calorimeter that fail the electron identification cuts. The number of such events with  $\cancel{E}_T > 25$  GeV is then scaled by the probability of a jet faking an electron, which is determined from multijet events with low  $\cancel{E}_T$ . The backgrounds due to multijet production where a jet fakes an isolated muon are determined by counting the number of events with muons that pass all cuts except the isolated muon requirement. This number of events is then multiplied by the probability that a jet will fake an isolated muon, which is determined from low jet multiplicity events where top and  $W$  events are negligible, but bottom and charm are present.

Backgrounds from  $W$  + jet production, which contain real isolated electrons and muons, are determined using the fact that QCD background processes follow an exponential scaling law in the number of observed jets.<sup>8</sup> This leads to the approximate prediction:

$$\frac{N_n}{N_{n-1}} = \text{constant}, \quad (1)$$

where  $N_n$  is the number of lepton +  $n$ -jet events and  $N_{n-1}$  is the number of lepton +  $(n-1)$ -jet events. QCD multijet events and  $Z$  + jets events in our data are consistent with this assumption. Since  $W$  + jets production is also a QCD process, these events are predicted to follow this law as well, and, as can be seen from Fig. 7, they do to within the limit of available statistics. The slope of the line in Fig. 7 is then used to determine the number of  $W$  + four jet events in our sample before the  $\mathcal{A}$  and  $H_T$  cuts. A 20% systematic uncertainty is assigned to the slope of the line, determined from difference in the slopes of the  $W$  + jets events and the multijet events. The  $Z$  and  $W$  slopes agree within statistics. The fraction of  $W$  + four jet events passing the  $\mathcal{A}$  and  $H_T$  cuts is determined from Monte Carlo simulations.

We check the calculated backgrounds by fitting the observed distribution of events in the  $\mathcal{A}$ ,  $H_T$  plane. We divide the  $\mathcal{A}$ ,  $H_T$  plane into four quadrants whose boundaries are defined by our  $\mathcal{A}$  and  $H_T$  cuts. The ratio of events of each type (top,  $W$  + jets, QCD fake + jets) in each quadrant is then taken from Monte Carlo or the fake electron data. The overall number of events of each type is determined by fitting the observed distribution. See Fig. 8. The results for the backgrounds agree with those obtained using the scaling law.

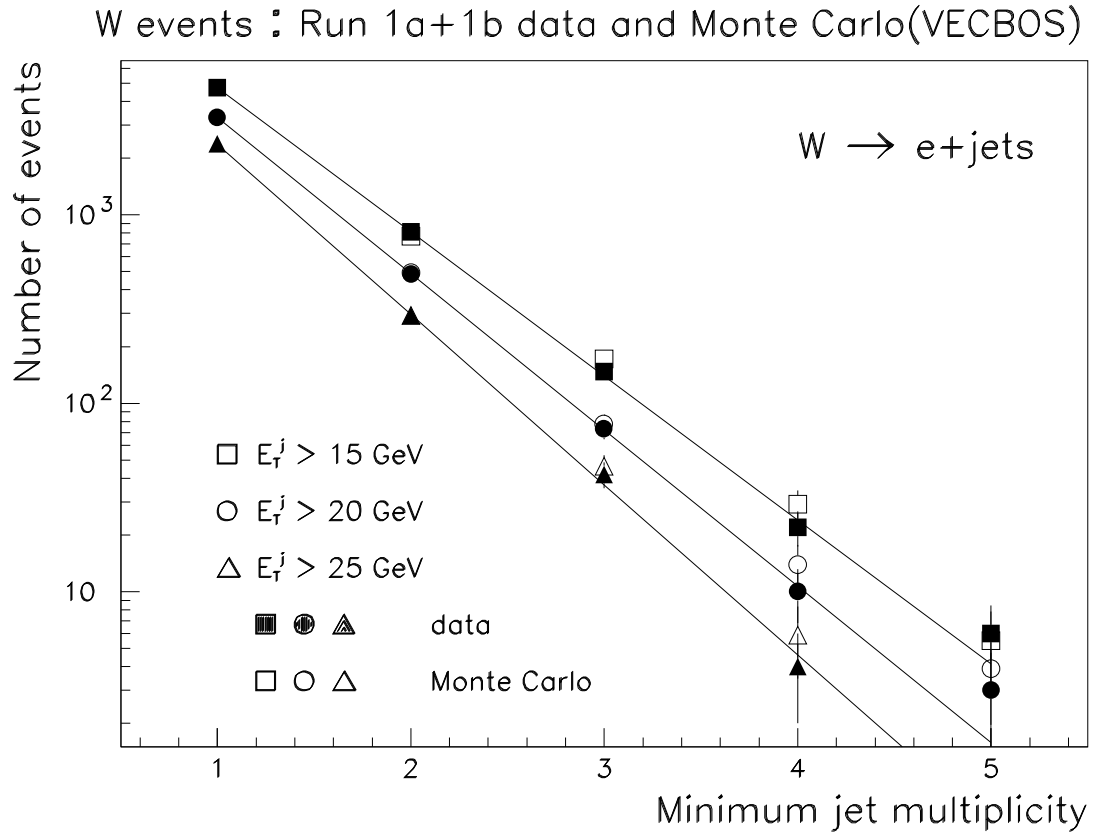


Figure 7: Plot of number of  $W + \text{jets}$  events as a function of jet multiplicity before  $\mathcal{A}$  and  $H_T$  cuts.



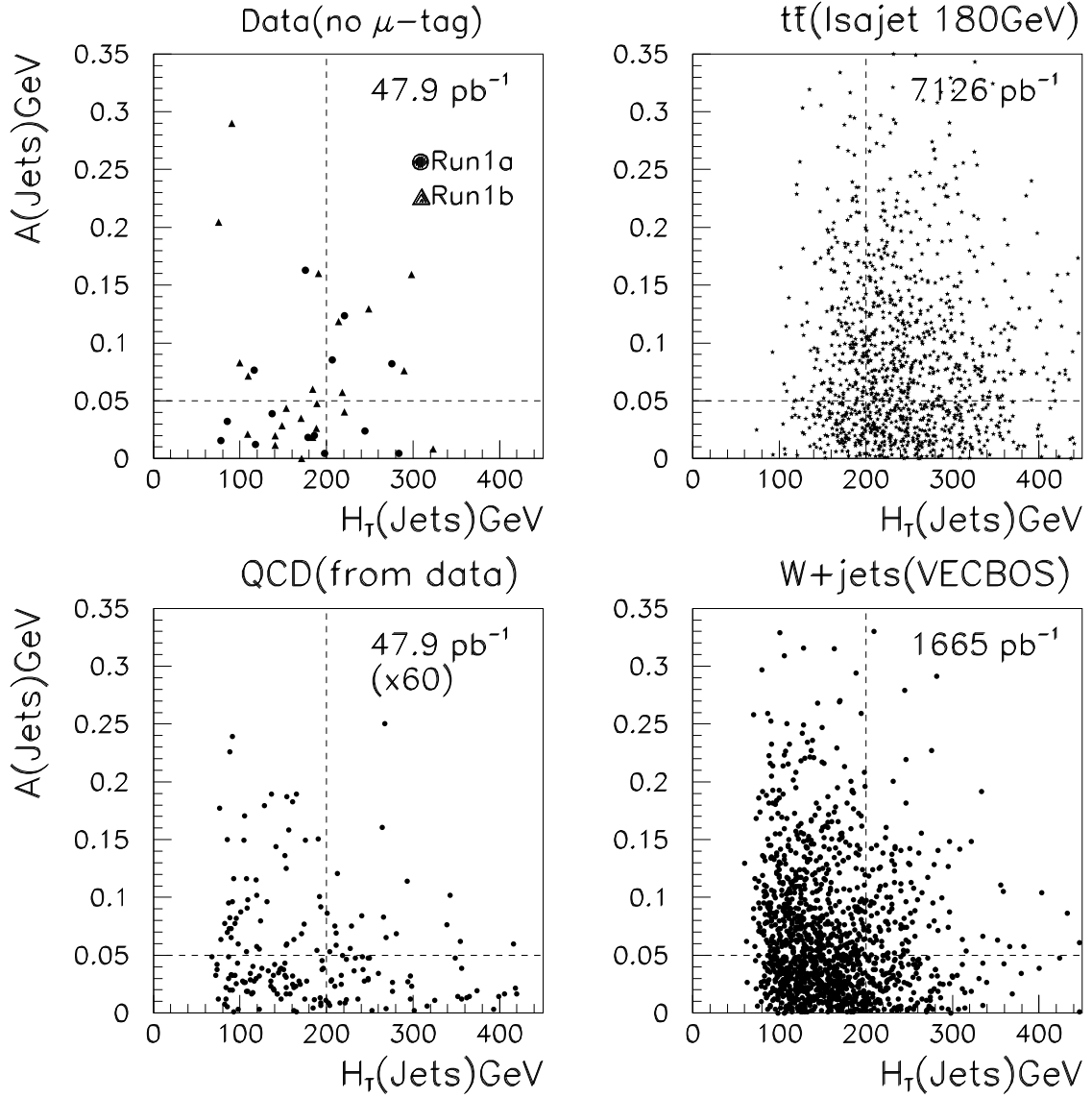


Figure 8:  $\mathcal{A}$  vs  $H_T$  distribution for data,  $t\bar{t}$  events,  $W$  + jet events and QCD multijet events.

Table 2: Summary of number of events observed, the predicted background, and the probability for the background to account for the data for both standard and loose cuts. A  $t\bar{t}$  production cross section ( $\sigma_{t\bar{t}}$ ) is also given for a top quark mass ( $M_t$ ) of 200 GeV/c<sup>2</sup>.

	Standard Selection	Loose Selection
Dileptons	3	4
Lepton + Jets (Shape)	8	23
Lepton + Jets (Muon tag)	6	6
All channels	17	33
Background	$3.8 \pm 0.6$	$20.6 \pm 3.2$
Probability	$2 \times 10^{-6}$ ( $4.6\sigma$ )	0.023 ( $2.0\sigma$ )
$\sigma_{t\bar{t}} (M_t = 200 \text{ GeV}/c^2)$	$6.3 \pm 2.2 \text{ pb}$	$4.5 \pm 2.5 \text{ pb}$

The results from the lepton + jets channels without muon tagging are listed in Table 2. With the standard cuts, the total number of untagged  $e + \text{jets}$  and  $\mu + \text{jets}$  events is 8 with a background of  $1.9 \pm 0.5$  events. The probability of an upward fluctuation of background having resulted in the observed signal is 0.002 ( $2.9 \sigma$ ). The cross section from the lepton + jets channels is  $4.9 \pm 2.5 \text{ pb}$ . With the loose cuts ( $\mathcal{A} > 0.03$  and no  $H_T$  cut), the total number of  $e + \text{jets}$  and  $\mu + \text{jets}$  events is 23 with a background of  $15.7 \pm 3.1$  events. This corresponds to a cross section of  $4.0 \pm 3.2 \text{ pb}$ . The agreement in the cross section calculated with the standard and loose cuts indicates that our backgrounds are correctly accounted for within the limits of statistics.

## 5 Lepton + Jets with $b$ quark tag

By requiring the presence of a  $b$  quark jet in our events, we can substantially reduce the major backgrounds. We tag  $b$  events by requiring a muon to be located within 0.5 in  $\eta$ - $\phi$  space of a jet in the event, and to have a minimum  $P_T$  of 4 GeV. For the lepton + jets channel without tags, we require that no such muons be present. The two sets of channels are then independent.

Standard Model  $t\bar{t}$  events that decay according to the lepton + jets signature contain, after the decays of the top quarks and the  $W$ 's, 2  $b$  quarks and approx-

imately 2.5  $c$  quarks. Each  $b$  or  $c$  has a branching ratio into a muon of about 10%. Thus, 44% of the  $t\bar{t}$  lepton + jets events contain a muon from a  $b$  or  $c$  decay. The DØ muon system acceptance and detection efficiency (about 45%) is such that about 20% of the  $t\bar{t}$  events have a detectable muon tag. The kinematic requirements on the lepton + jets with muon tag events are given in Table 1. The loose kinematic cuts are the same as the standard cuts, except the cut on  $H_T$  is not used.

Backgrounds are calculated by multiplying the observed number of  $W$  + jets events and multijet events with a fake lepton by the fraction of background events containing muon tags. As can be seen in Fig. 9, the tagging rate is consistent with being proportional to the number of jets, as would be expected if heavy quarks from gluon splitting and fakes dominate the background. Corrections are made for the change in the tagging probability with jet  $E_T$  and event  $\cancel{E}_T$ .

The results from the lepton + jets with muon tag channels are listed in Table 2. With the standard cuts, the total number of  $e$  + jets and  $\mu$  + jets with muon tag events is 6 with a background of  $1.2 \pm 0.2$  events. The probability of an upward fluctuation of background having resulted in the observed signal is 0.002 ( $2.9 \sigma$ ). The cross section from the lepton + jets channels with tag is  $8.9 \pm 4.8$  pb. With the loose cuts (no  $H_T$  cut), the total number of  $e$  + jets and  $\mu$  + jets events is also 6 with a background of  $2.2 \pm 0.3$  events. The cross section for the loose cuts for the lepton + jets channels with muon tag is  $6.3 \pm 4.2$  pb. Here again, we assume a top mass of 200 GeV/ $c^2$ . The agreement in the cross section calculated with the standard and loose cuts indicates that our backgrounds are correctly accounted for within the limits of statistics. In Fig. 10, we show the distribution of loose cut events after the QCD background contribution has been subtracted compared with the  $W$  + jets background. The excess of events for jet multiplicities greater than two is clear.

## 6 Cross Section and Significance

Combining the above seven channels, we observe a total of 17 events with an expected background of  $3.8 \pm 0.6$  events. The probability of an upward fluctuation of the background giving 17 or more events is  $2 \times 10^{-6}$ . This corresponds to a 4.6 standard deviation effect for a Gaussian probability distribution. Our measured cross section plotted as a function of assumed top quark mass is shown in Fig. 11.

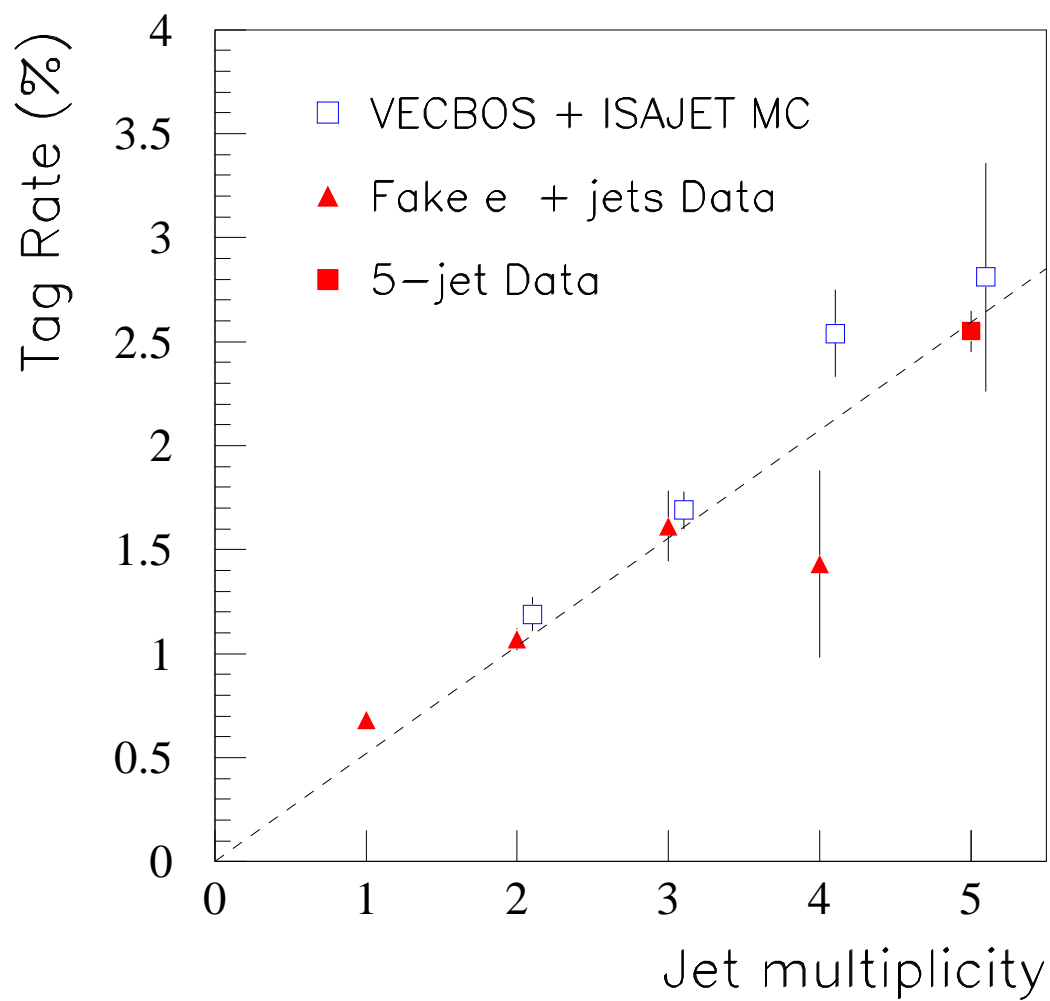


Figure 9: Muon tag rate for background events as a function of jet multiplicity.

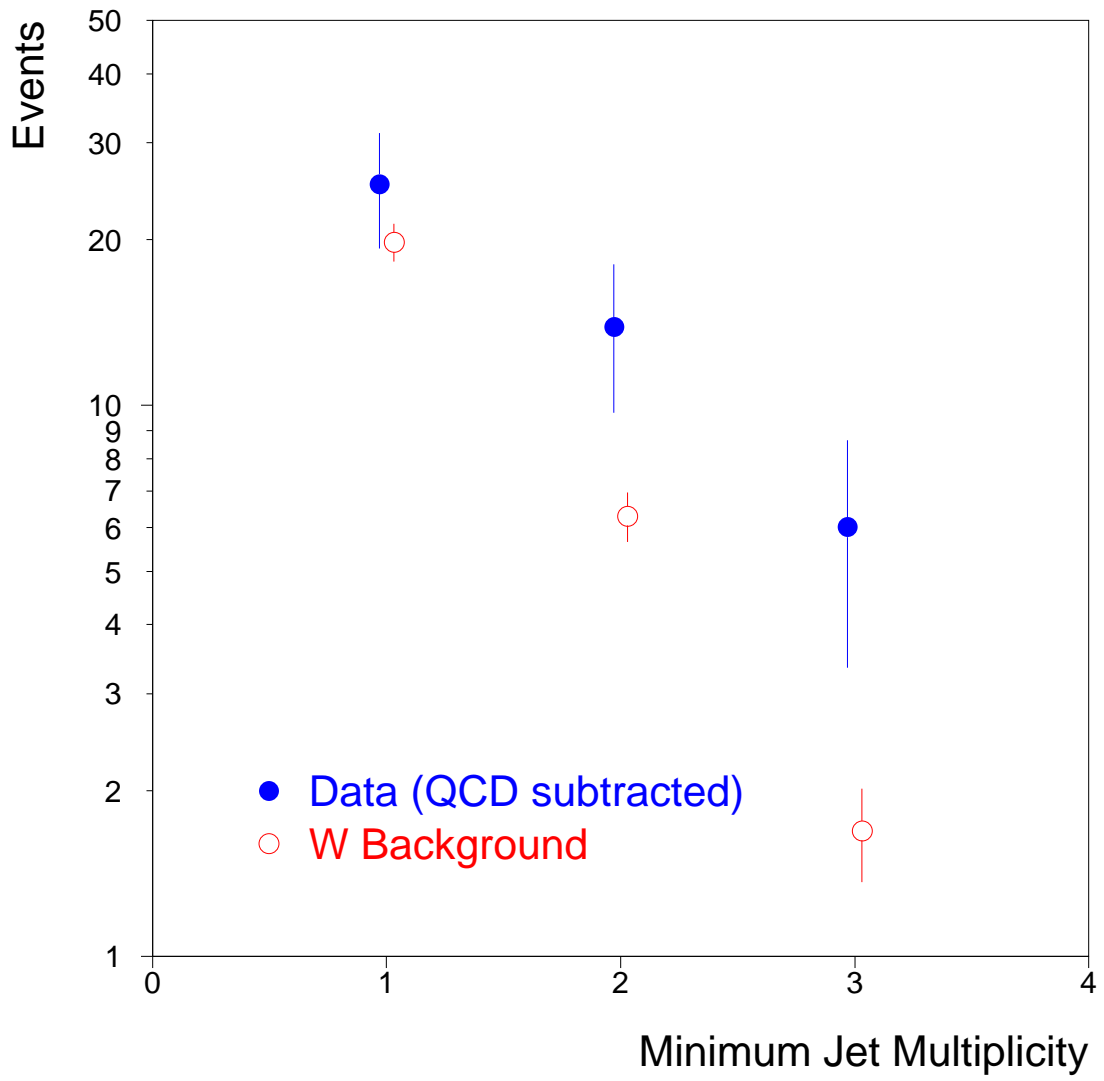


Figure 10: Plot of lepton + jets + muon tag events as a function of inclusive jet multiplicity.

Also shown is a theoretical cross section curve.<sup>9</sup> Assuming a top quark mass of 200 GeV/c<sup>2</sup>, our measured cross section is  $6.3 \pm 2.2$  pb. The error in the cross section includes a 12% uncertainty in the integrated luminosity. We have included the difference in top detection efficiencies when using the HERWIG<sup>10</sup> Monte Carlo instead of ISAJET in the systematic error. For the loose cuts, we observe a total of 33 events with a expected background of  $20.6 \pm 3.2$  events. This leads to a cross section of  $4.5 \pm 2.5$  pb for a 200 GeV/c<sup>2</sup> top mass for the loose cuts, in good agreement with the value obtained from the standard cuts. Figure 12 shows the cross sections for the various decay channels calculated individually. We have calculated the probability of seeing our distribution of events across the seven channels and find that our result is consistent with the expected top branching fractions at the 53% confidence level. (Note that the branching fractions are determined by the assumption of top decay to  $W + b$ , and the Standard Model  $W$  branching fractions.) We observe a statistically significant excess of events, and the distribution of these events among the decay channels studied is consistent with top quark production. We conclude that we observe the top quark.

We also have results from searches using multivariate techniques and from searches in the channel where both  $W$ 's decay to jets. Details of these analyses can be found in the references<sup>11,12</sup>.

## 7 Mass Analysis

Having determined that there is an excess of events in our data, and that the observed distribution of events is consistent with that expected from the Standard Model top quark, we now study the kinematic properties of our lepton + jets events in order to determine the top quark mass.

We assume that our excess events are due to the process

$$t\bar{t} \rightarrow (W^+b)(W^-\bar{b}) \rightarrow (l\nu b)(q\bar{q}\bar{b}).$$

Using both  $W$  mass constraints, and requiring that the masses of the  $t$  and  $\bar{t}$  quarks be equal, we perform a two constraint (2C) kinematic fit for the top quark mass. We select lepton + jet events requiring at least 4 jets with  $E_T > 15$  GeV and  $|\eta| < 2.5$ . We use jets of cone radius 0.3. We use only the four highest  $E_T$  jets in the fit. For each event, there are 12 distinct ways of assigning jets to the

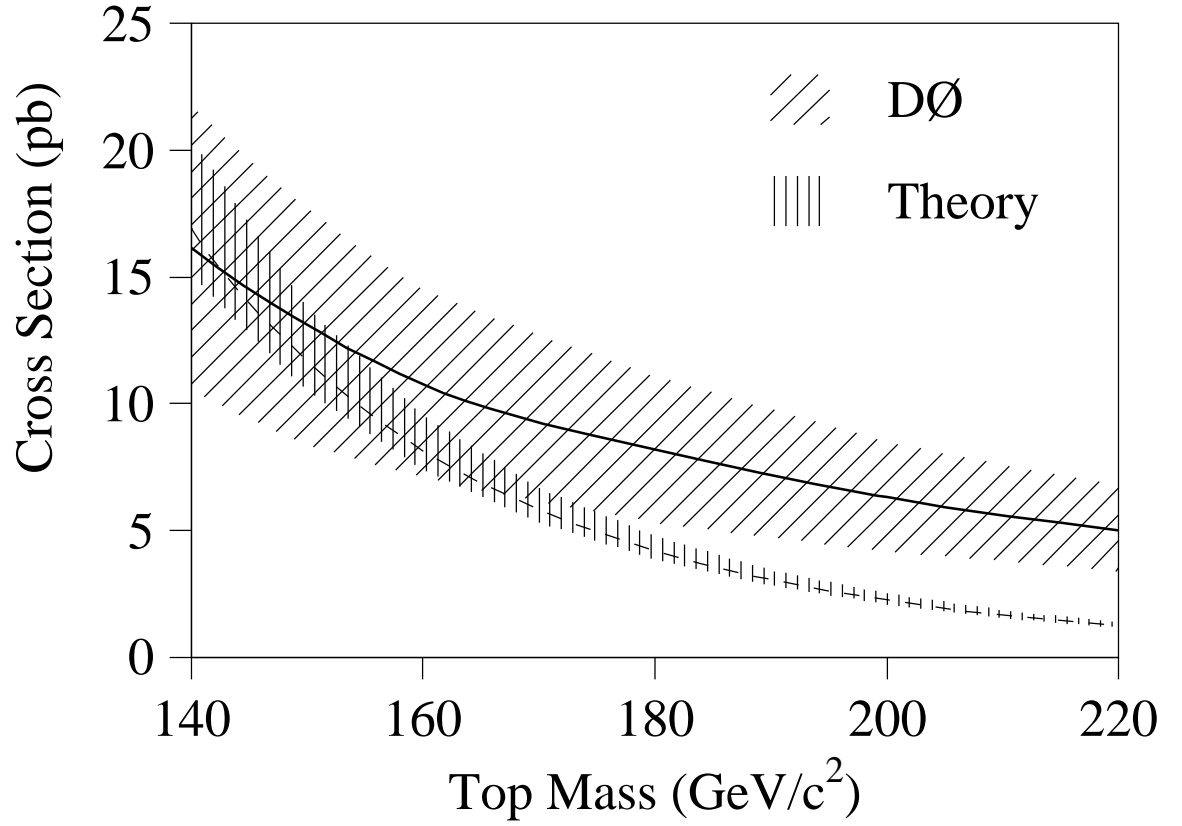


Figure 11: Measured  $t\bar{t}$  production cross section as a function of assumed top quark mass. Also shown is the theoretical cross section curve.

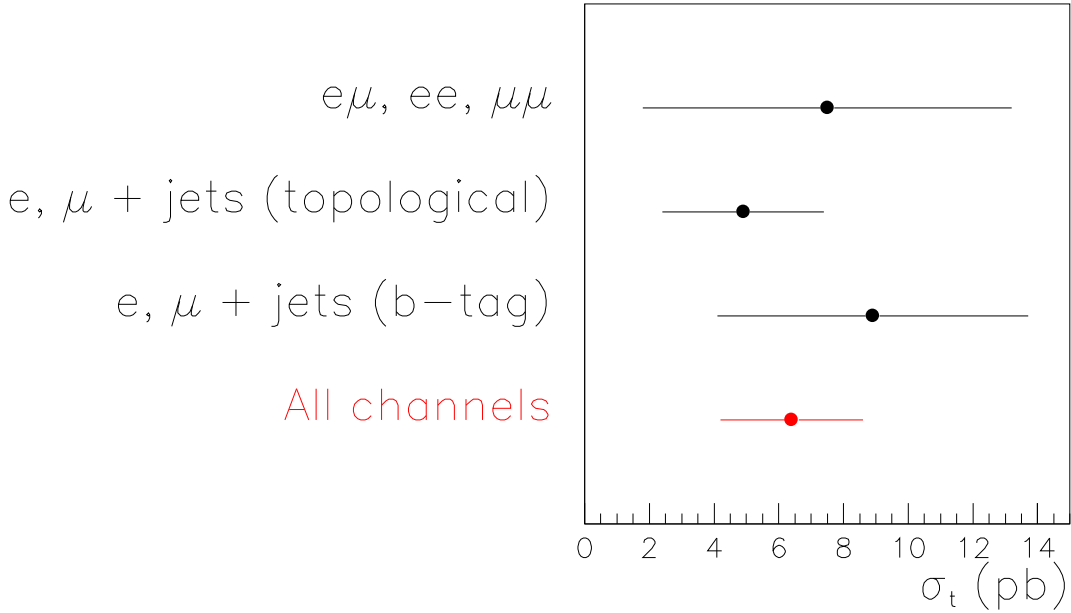


Figure 12: Measured  $t\bar{t}$  production cross section as a function of decay mode for 200 GeV/c<sup>2</sup> assumed top quark mass.

original partons. We use up to three combinations with  $\chi^2 < 7$  and calculate a  $\chi^2$  weighted average mass for each event.

We have performed extensive Monte Carlo studies of the method and tested many possible variations. For example, we tested using just the best  $\chi^2$  combination instead of the weighted average of the three best for each event and found that the weighted average method gave slightly better results. We tested our jet energy corrections by studying  $Z + \text{jet}$  events where the  $Z$  decays to  $e^+e^-$  and comparing the  $E_T$  of the  $Z$  with the  $E_T$  predicted from the jets. As shown in Fig. 13, after jet corrections,  $E_T$  is well balanced in our events. Jets with a tag muon have twice the muon  $p_T$  added to the jet energy to compensate for muon and the missing neutrino.

We have studied in detail the effects of initial state radiation (ISR), final state radiation (FSR), and the combinatorical background due to the wrong combinations. Note that the solution with the lowest  $\chi^2$  corresponds to the correct jet assignment less than 20% of the time. Figure 14 shows the effects of wrong jet assignment, and QCD radiation on our mass resolution for 180 GeV/c<sup>2</sup> top events generated with the ISAJET and HERWIG Monte Carlos.



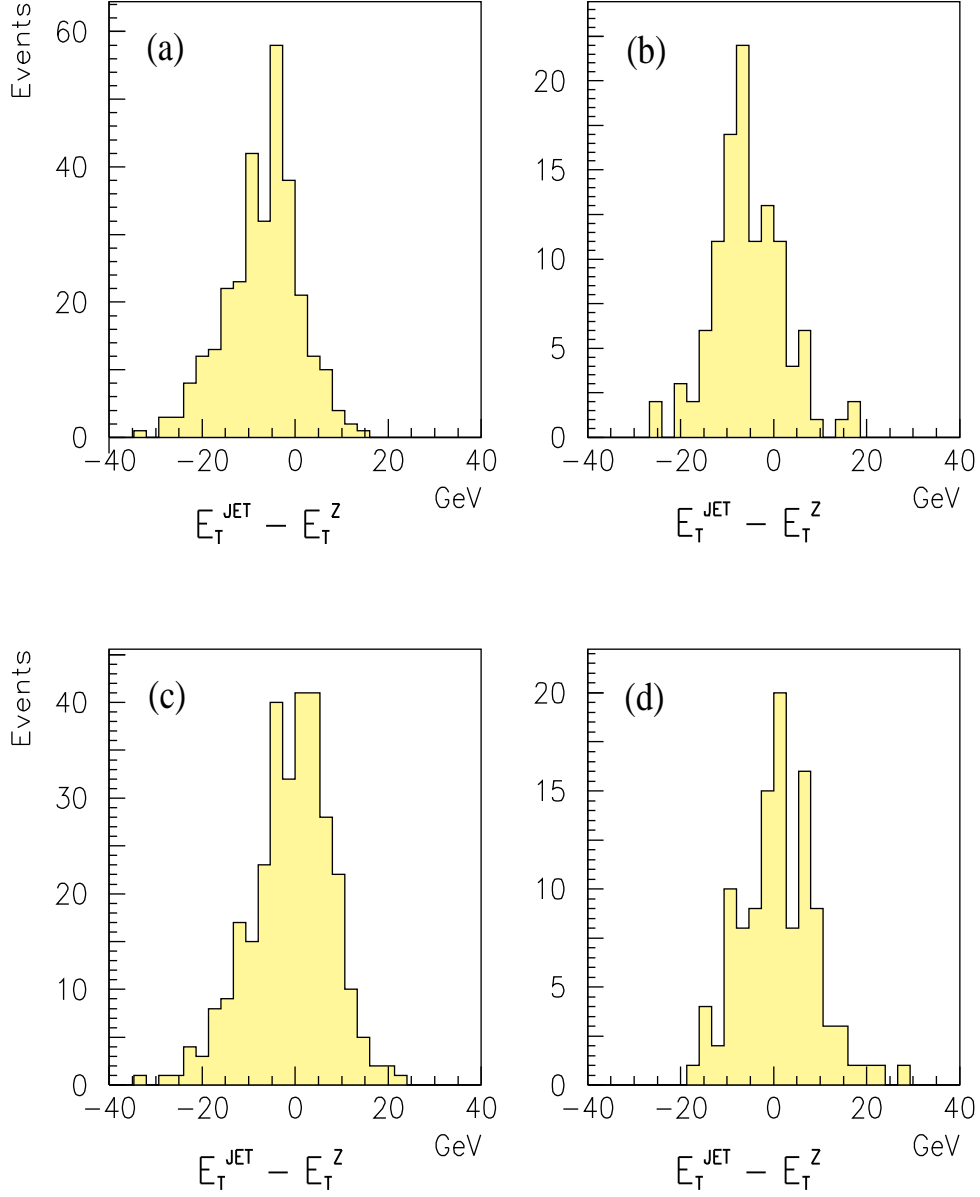


Figure 13:  $E_T^{\text{jet}} - E_T^Z$  for (a) Monte Carlo before final jet energy corrections, (b) data before final jet energy corrections, (c) Monte Carlo after all jet energy corrections and (d) data after all jet energy corrections.

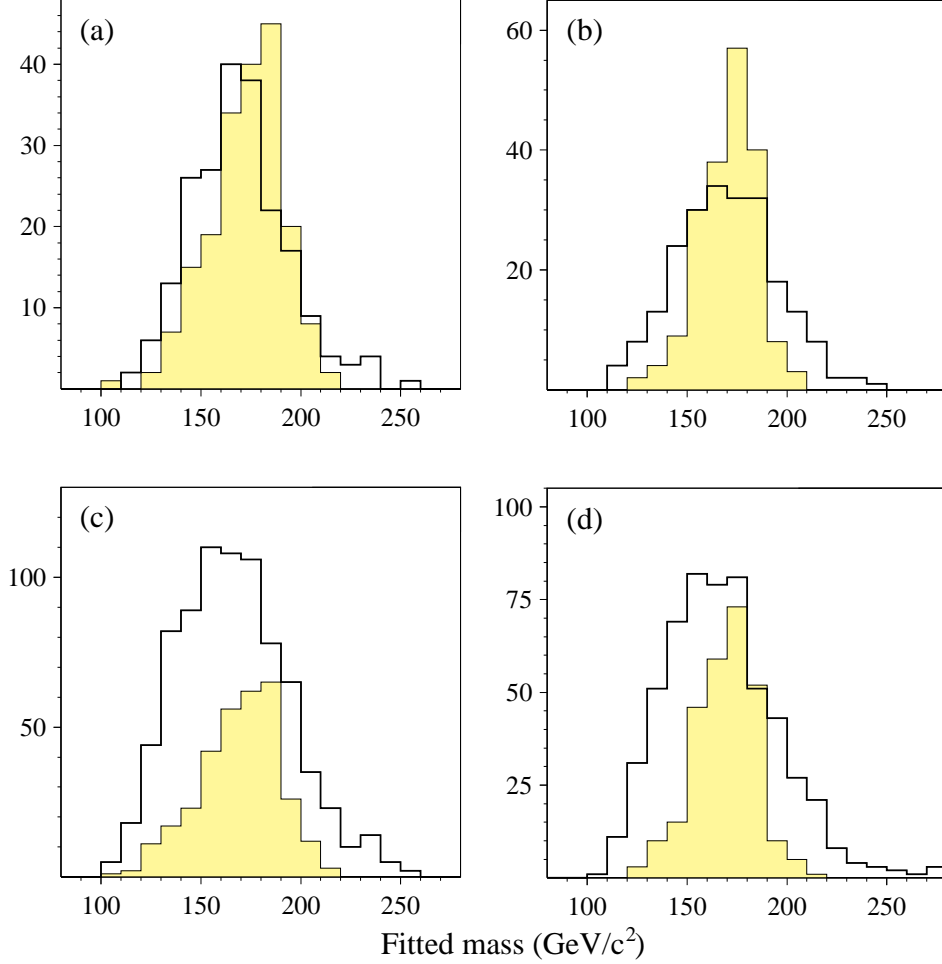


Figure 14: Distributions of fitted top quark mass for (a,c) ISAJET and (b,d) HERWIG 180  $\text{GeV}/c^2$  top Monte Carlo. In (a) and (b), events have exactly four jets, uniquely matched to the four primary jets (two  $b$  jets + two  $W$  jets) required for mass analysis. In (b) and (d), four or more jets are allowed as in actual analysis, without any matching requirement. Open histograms show the fitted top quark mass as in actual analysis. Shaded histograms show the fitted mass for the correct jet assignment for those events in which the four highest  $E_T$  jets are uniquely matched to the four primary jets.

We apply our kinematical fitting procedure to ISAJET Monte Carlo top events with a full GEANT detector simulation to obtain resolution functions for different assumed top masses. These distributions are shown in Fig. 15 for a range of top mass values from 140 to 240 GeV/c<sup>2</sup>. Note that the average value of the calculated mass is shifted from the input mass due to the effects of ISR, FSR and jet assignment combinatorics. The Monte Carlo top mass distributions are then fit; the fits are smoothed and parametrized as a continuous function of top mass. The mass distributions from background events are obtained by applying the same kinematic fit to  $W + \text{jet}$  events from VECBOS<sup>13</sup> and QCD multijet events obtained from the bad electron sample.

Eleven of the 14 lepton + jets candidate events selected using the standard cuts were successfully fit. Figure 16 shows the mass distribution, along with the likelihood distribution from the fit. A maximum likelihood fit is then used to extract the top mass from our data. The likelihood fit gives a top mass of  $199^{+31}_{-25}$  GeV/c<sup>2</sup> and describes the data well. To increase the statistics available for the fit and to test for any possible bias from the  $H_T$  cut, we also performed the mass analysis on events selected using the loose requirement. Out of the 27 loose lepton + jets events that have at least four jets, 24 were successfully fit. The likelihood fit to the loose sample gave a value of  $199^{+19}_{-21}$  GeV/c<sup>2</sup> for the top mass. The statistical uncertainty is smaller for the loose cuts, since the  $H_T$  cut used in the standard analysis biases the fitted mass distributions. The events are shown in Fig. 16, along with the likelihood distribution from the fit. The results of the fit did not depend significantly on whether or not the background normalization was constrained to the calculated value. As can be seen in Fig. 16, The masses of the tagged events are consistent with those of the untagged events. Using HERWIG instead of ISAJET resulted in a 195 GeV/c<sup>2</sup> value for the top mass. The systematic uncertainty on the top mass is  $^{+14}_{-21}$  GeV/c<sup>2</sup> and is dominated by the uncertainty in the jet energy scale.<sup>14</sup>

Figures 17 and 18 give preliminary results for the transverse momentum distribution and  $t\bar{t}$  mass distribution for top candidate events that pass the standard cuts. Within the limits of the low statistics, the observed distributions are in agreement with the expected mixture of Standard Model top plus background events.

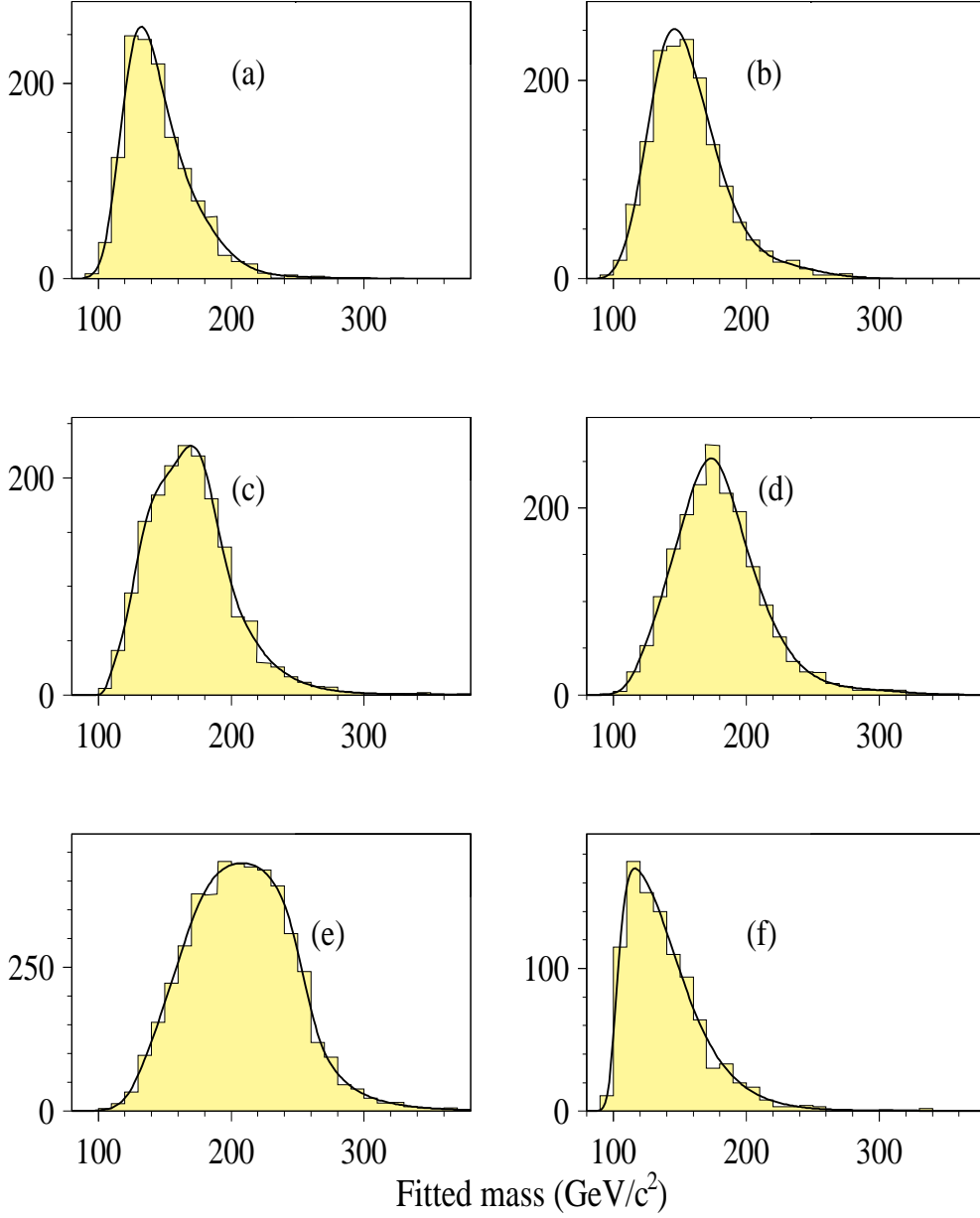


Figure 15: Results of Kinematic fit for top mass for ISAJET Monte Carlo events (a) 140  $\text{GeV}/c^2$  top , (b) 160  $\text{GeV}/c^2$  top, (c) 180  $\text{GeV}/c^2$  top, (d) 200  $\text{GeV}/c^2$  top. (e) 240  $\text{GeV}/c^2$  top, and (f) for  $W$  + four jet Monte Carlo

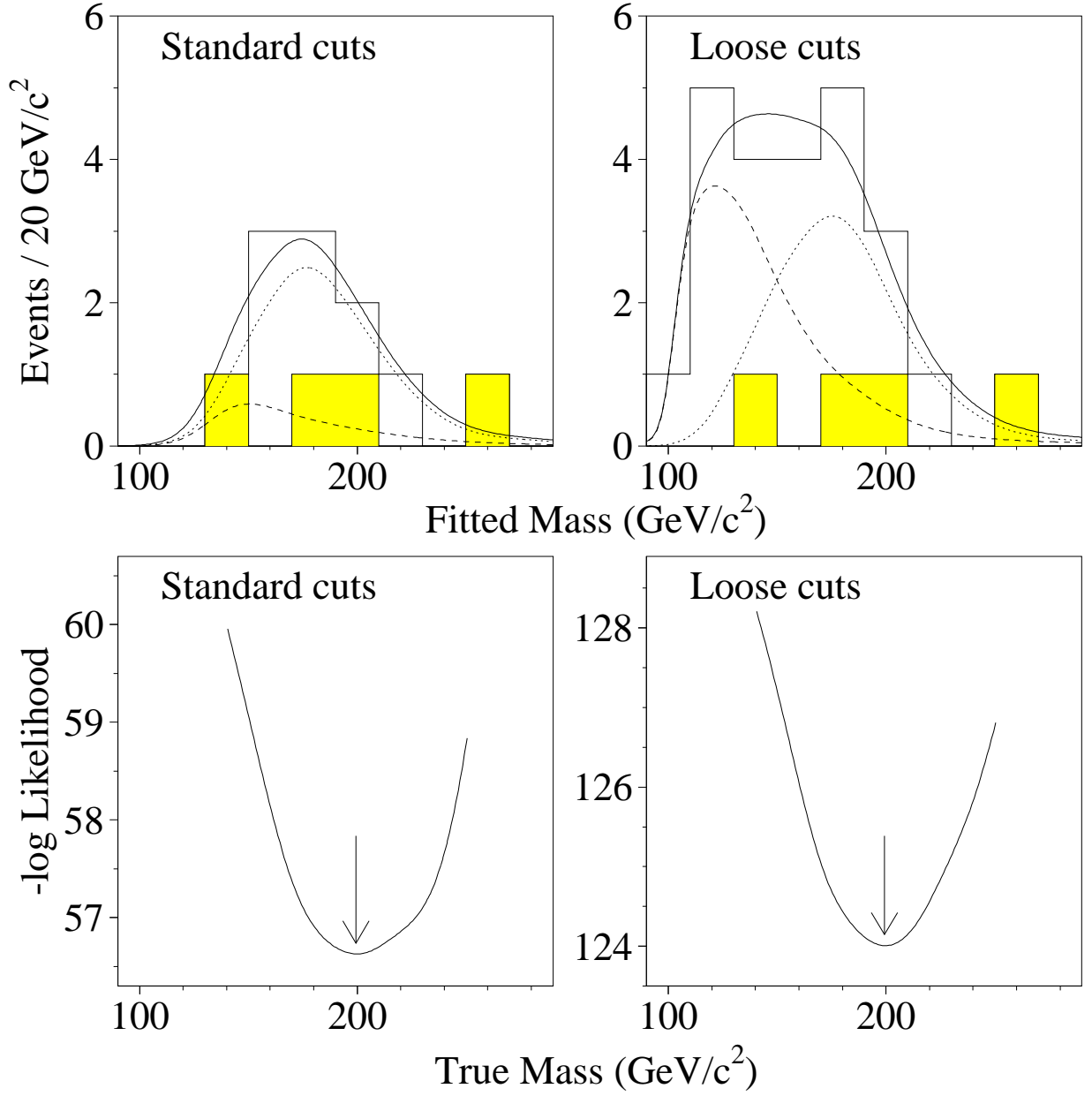


Figure 16: Top mass and likelihood distribution for the standard and loose cuts. The dashed line is the expected background distribution, the dotted line the expected distribution from 199  $\text{GeV}/c^2$  Monte Carlo top events, and the solid line the sum of top + background. The shaded events have tag muons.

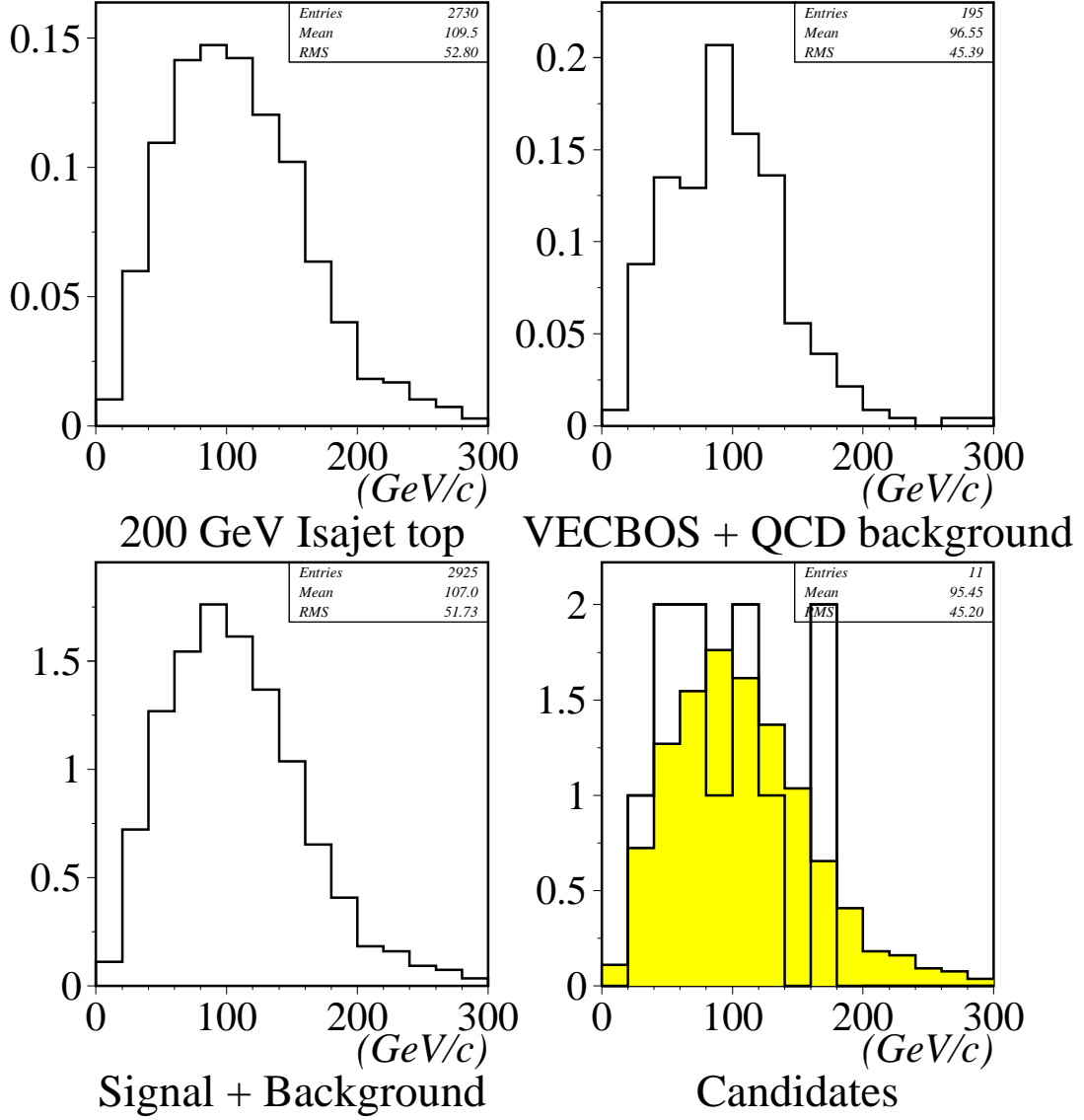


Figure 17: Top Transverse Momentum distribution for the standard cuts. The shaded region is the expected distribution of top plus background events normalized to the data.

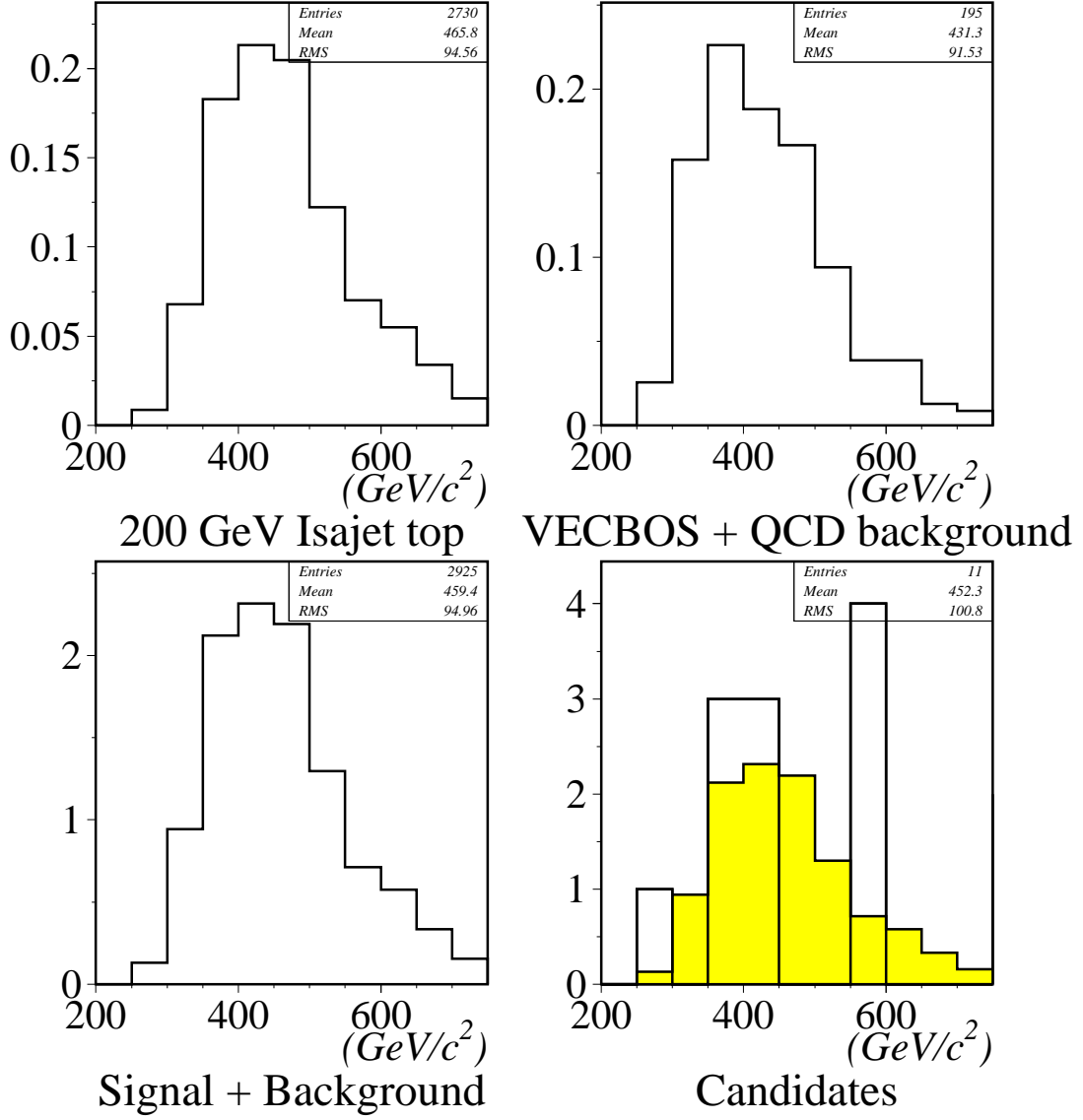


Figure 18:  $t\bar{t}$  mass distribution for the standard cuts. The shaded region is the expected distribution of top plus background events normalized to the data.

## 8 Hadronic $W$ Decays

Top events have two  $W$ 's in them, while the main backgrounds do not. In this section, we present preliminary results of a search in our single lepton data for evidence of  $W$  to two jet decays. We select events requiring the loose cuts and at least four jets. The jets are required to have  $|\eta| < 2.5$ . All jet assignments consistent with the muon tag (if one is present) are used. The solutions are weighted according to  $e^{-\chi^2/2}$  with  $\chi^2 \propto \ln^2(M(bl\nu)/M(bjj))$ . Each event's weights are normalized to unity. For the top mass, we plot the weighted average of the  $bl\nu$  mass and the  $bjj$  mass. When the  $b$  jet in  $t \rightarrow bjj$  is untagged, often the highest energy jet (jet 1) as measured in the top CM frame is assigned to the  $b$  jet and we plot  $M_{23}$  for the  $W$  mass. However, if  $(E_1 - E_2) < (E_2 - E_3)$  in the top CM frame, we plot  $M_{23}$  and  $M_{13}$  with equal weight. The dijet mass vs top mass distribution is shown in Fig. 19 for 200 GeV/ $c^2$  HERWIG top + background events and for background events only. The same plots for data events and for background events are shown in Fig. 20. Note that the data are inconsistent with the prediction for background alone. If we now plot the top mass for dijet masses greater than 58 GeV/ $c^2$  and the dijet mass for top masses greater than 150 GeV/ $c^2$ , we see both a peak in the top mass distribution consistent with 200 GeV/ $c^2$  top and a peak in the dijet mass consistent with  $W$  decays. See Fig. 21. We conclude that the events that are from the top signal region also show a  $W$  to dijet mass peak, as expected for top events.

## 9 Conclusion

We report the observation of the top quark with the DØ detector. We measure the top mass to be  $199^{+19}_{-21}(\text{stat.})^{+14}_{-21}(\text{syst.})$  GeV/ $c^2$  and measure the production cross section to be  $6.4 \pm 2.2$  pb at our central mass. We show the existence of a peak in the dijet mass distribution consistent with hadronic decays of the  $W$  in our top data. Note that by the time these proceedings appear in print, we will have updated results from a data sample of approximately 100 pb $^{-1}$  which is twice as large as that discussed here. An upgraded version of the DØ detector will run in 1999 and we expect to begin making detailed measurements of the properties of the top quark with a data sample of 2 fb $^{-1}$  at that time.

I would like to thank all of my colleagues on the DØ experiment whose efforts



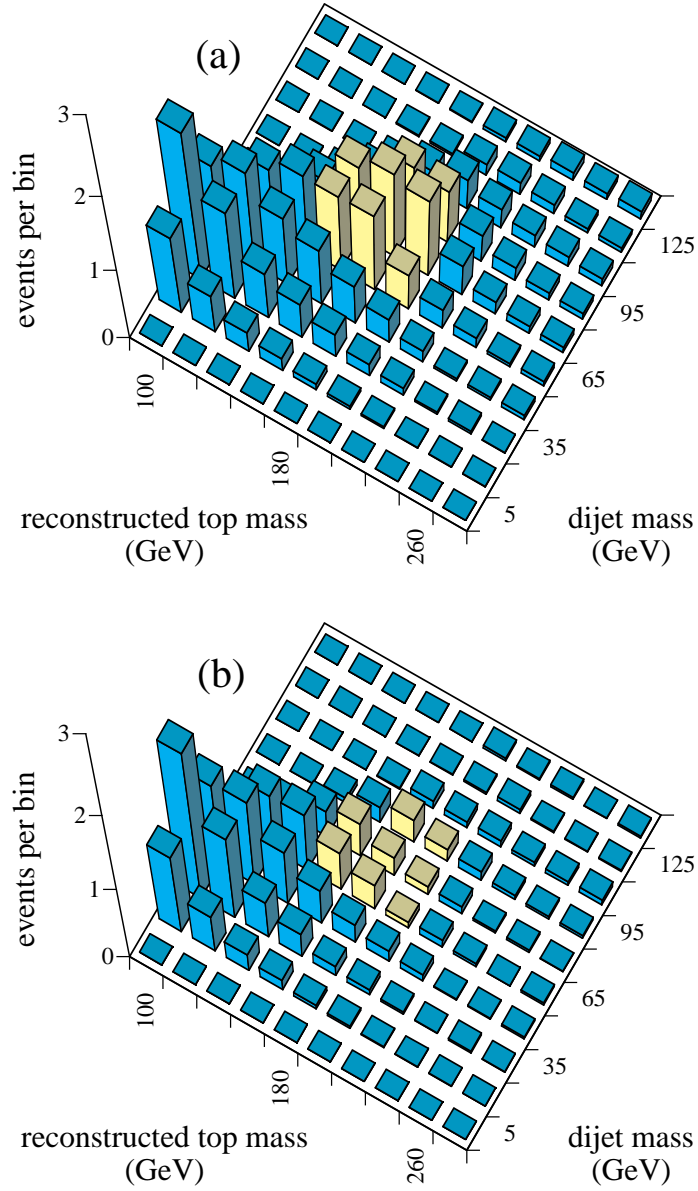


Figure 19: Lego distributions in reconstructed top quark mass and dijet mass of (a) sum of HERWIG 200 GeV/ $c^2$  top Monte Carlo and background events; (b) background alone. The background includes both  $W + \text{four jet}$  VECBOS Monte Carlo and QCD multijet data, each normalized using control samples. The events usually increment more than one bin because of multiple solutions; the increments for each event are normalized so that they sum to unity.

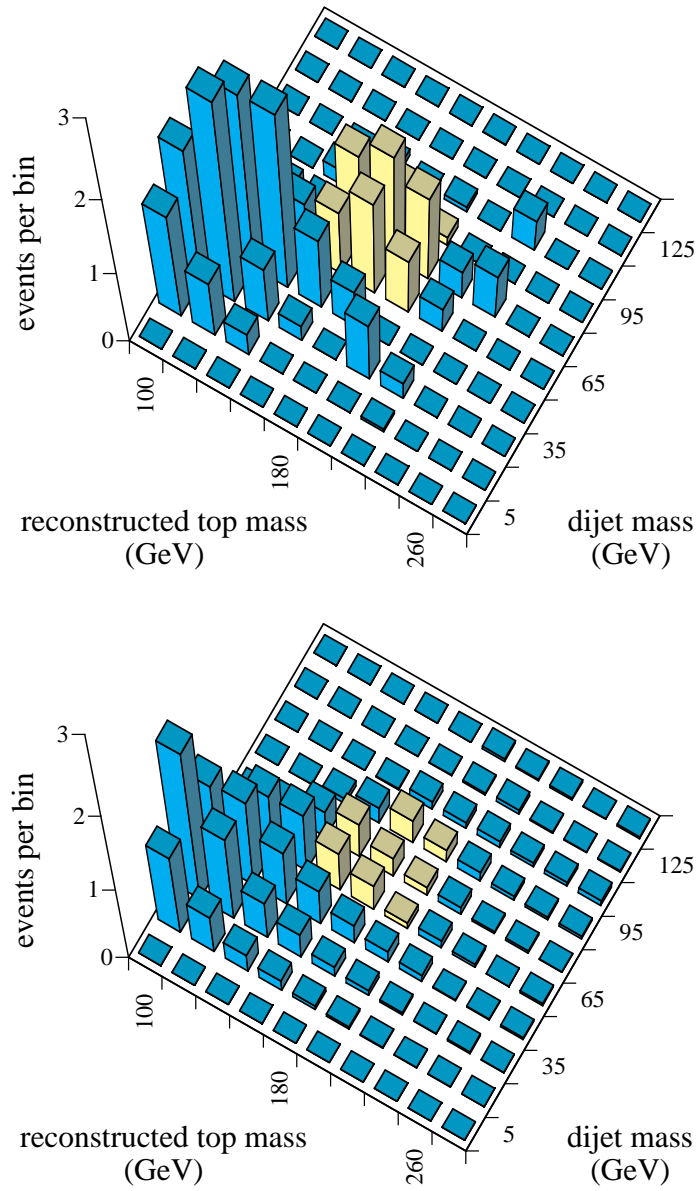


Figure 20: Lego distribution in reconstructed top quark mass and dijet mass of the data (26 events). The events usually increment more than one bin because of multiple solutions; the increments for each event are normalized so that they sum to unity. The background only distribution from Fig. 19(b) is reproduced below for comparison.

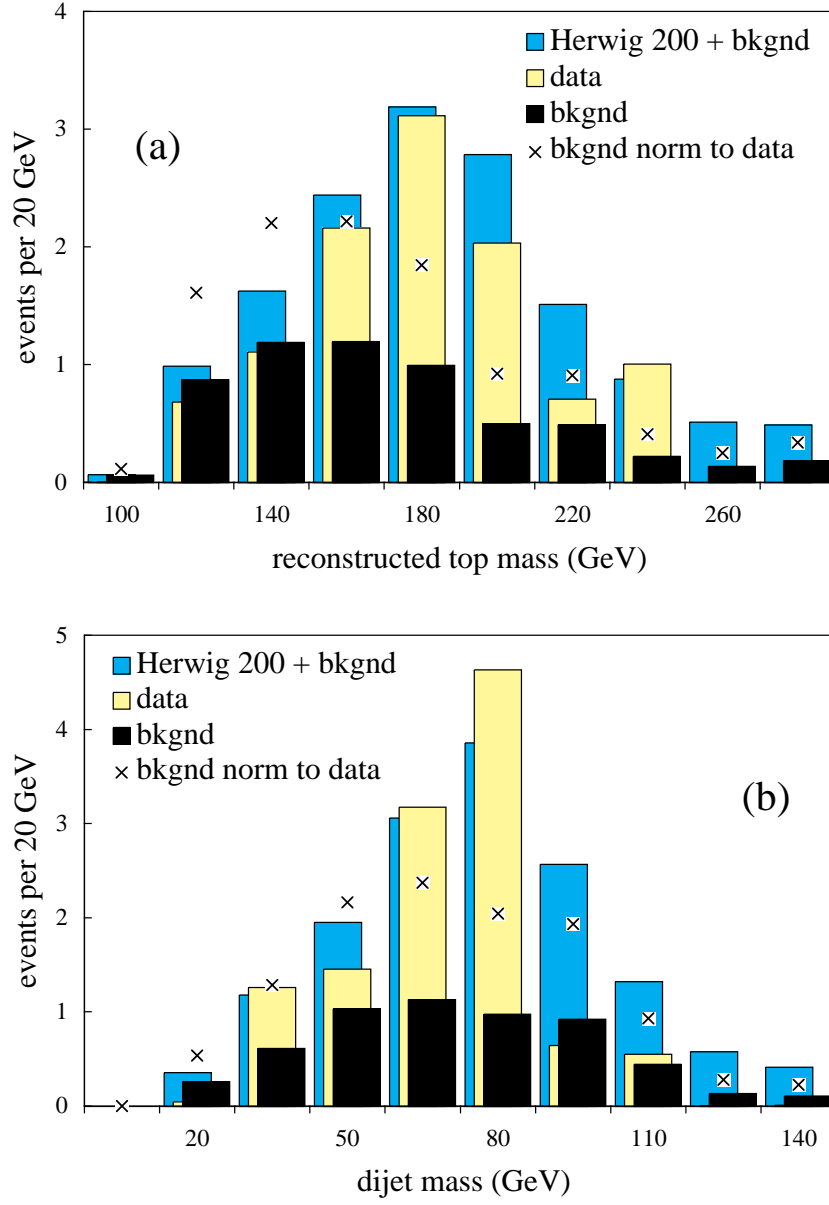


Figure 21: Distributions of (a) reconstructed top quark mass  $M_t$  and (b) dijet mass  $M_{jj}$  with (a)  $M_{jj} > 58 \text{ GeV}/c^2$  and (b)  $M_t > 150 \text{ GeV}/c^2$ , for (light shaded) data, (medium) sum of background and HERWIG 200  $\text{GeV}/c^2$  top Monte Carlo, (black) background alone, and (X's) background normalized to match the area of the data.

made these results possible.

DØ thanks the Fermilab Accelerator, Computing, and Research Divisions, and the support staffs at the collaborating institutions for their contributions to the success of this work. We also acknowledge the support of the U.S. Department of Energy, the U.S. National Science Foundation, the Commissariat à L’Energie Atomique in France, the Ministry for Atomic Energy and the Ministry of Science and Technology Policy in Russia, CNPq in Brazil, the Departments of Atomic Energy and Science and Education in India, Colciencias in Colombia, CONACyT in Mexico, the Ministry of Education, Research Foundation and KOSEF in Korea and the A.P. Sloan Foundation.

## References

- [1] S. Abachi *et al.*, (DØ Collaboration), Phys. Rev. Lett. **74**, 2632 (1995).
- [2] F. Abe *et al.*, (CDF Collaboration), Phys. Rev. Lett. **74**, 2626 (1995).
- [3] S. Abachi *et al.*, (DØ Collaboration), Phys. Rev. Lett. **72**, 2138 (1994).
- [4] S. Abachi *et al.*, (DØ Collaboration), Phys. Rev. Lett. **74**, 2422 (1995).
- [5] F. Abe *et al.*, (CDF Collaboration), Phys. Rev. D **50**, 2966 (1994); Phys. Rev. Lett. **73**, 225 (1994).
- [6] F. Paige and S. Protopopescu, BNL Report No. BNL38034, 1986 (unpublished), release v 6.89.
- [7] F. Carminati *et al.*, “GEANT Guide”, CERN Library, 1991 (unpublished).
- [8] F.A. Berends *et al.*, Phys. Lett. **357B**, 32 (1991).
- [9] E. Laenen, J. Smith, and W. van Neerven, Phys. Lett, **321B**, 254 (1994).
- [10] G. Marchesini *et al.* Comput. Phys. Commun **67**, 465 (1992).
- [11] P. C. Bhat (DØ Collaboration), Proceedings of the 8th meeting of the Division of Particles and Fields of the APS, Vol. 1, p. 705, 1994; FERMILAB-CONF-95-211-E. To be published in the Proceedings of 10th Workshop on  $p\bar{p}$  Collider Physics, Fermilab, Batavia, IL, May 9–13, 1995.
- [12] B. Klima (DØ Collaboration), FERMILAB-CONF-95/303-E. To be published in the Proceedings of the 17<sup>th</sup> International Symposium on Lepton-Photon Interactions, Beijing, China, Aug. 10–16, 1995.

- [13] W. Giele, E. Glover, and D. Kosower, Nucl. Phys. **B403**, 633 (1993).
- [14] S. Snyder (DØ Collaboration), to be published in the Proceedings of the International Europhysics Conference on High Energy Physics, Brussels, Belgium July 1995 and M. Strovink (DØ Collab.), to be published in the Proceedings of 10th Workshop on  $p\bar{p}$  Collider Physics, Fermilab, Batavia, IL, May 9–13, 1995.